Error estimates of the Non-Intrusive Reduced Basis 2-grid method with parabolic equations

CANUM 2022

Elise Grosjean [1]
Yvon Maday [1]

[1] Jacques-Louis Lions laboratory
Sorbonne Université

30.05.2022 - 02.06.2022

Purpose

Reduce the computational costs of parameter-dependent problems with Non-Intrusive Reduced Basis methods eDF

SAFRAN

C|T
ingenierie

CADLM
TRANSFORMING DATA INTO INTELLIGENCE

cemosis
Centre de modélisation et de simulation de Strasbourg

MINES ParisTech | PSL

Scilab

JJL

Introduction to the NIRB methods

Reduced basis methods

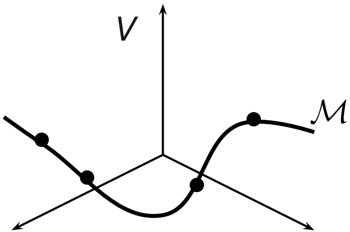

Figure: Solution manifold

$$\mathcal{M} = \{u(\mu) \in V |\ \mu \in \mathcal{G}\} \subset V.$$

- Parameter: $\mu \in \mathcal{G}$,
- Solution: $u(\mu) \in V$.

Introduction to the NIRB methods

Reduced basis methods

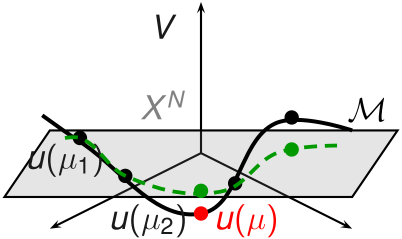

Figure: Solution manifold

$$\mathcal{M} = \{u(\mu) \in V | \ \mu \in \mathcal{G}\} \subset V.$$

- X^N Reduced basis space,
- Parameters $\mu_1, \dots, \mu_N \in \mathcal{G}$,
- Snapshots $u(\mu_1), \dots, u(\mu_N) \in V_h$,
- Projected snapshots onto X^N.
- Projected new solution onto X^N.

Introduction to the NIRB methods

Reduced basis methods

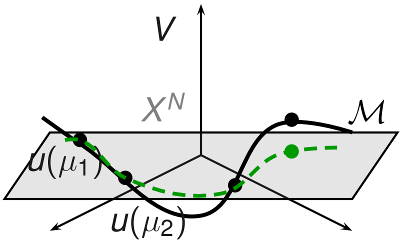

Figure: Solution manifold

$$\mathcal{M} = \{u(\mu) \in V | \ \mu \in \mathcal{G}\} \subset V.$$

- X^N Reduced basis space,
- Parameters $\mu_1, \dots, \mu_N \in \mathcal{G}$,
- Snapshots $u(\mu_1), \dots, u(\mu_N) \in V$,
- Projected snapshots onto X^N.

$$\inf_{\dim(X^N)=N} \operatorname{dist}(\mathcal{M}, X^N).$$

Kolmogorov n-width must be small [1] [2]

[1] P. Binev, A. Cohen, W. Dahmen, R. DeVore, G. Petrova, P. Wojtaszczyk *Convergence rates for greedy algorithms in reduced basis methods.* 2011.

[2] A. Buffa, Y. Maday, A.T. Patera, C. Prudhomme, and G. Turinici, *A Priori convergence of the greedy algorithm for the parameterized reduced basis.* 2012.

Introduction to the NIRB methods

Reduced basis methods

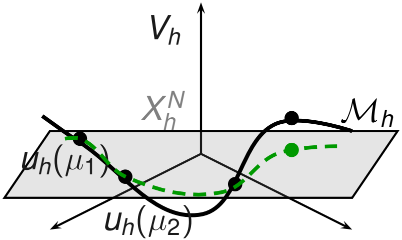

Figure: Solution manifold

$$\mathcal{M}_h = \{u_h(\mu) \in V_h \mid \mu \in \mathcal{G}\} \subset V_h.$$

- X_h^N Reduced basis space,
- Parameters $\mu_1, \ldots, \mu_N \in \mathcal{G}$,
- Snapshots $u_h(\mu_1), \ldots, u_h(\mu_N) \in V_h$,
- Projected snapshots onto X_h^N.

Kolmogorov n-width must be small [1] [2]

[1] P. Binev, A. Cohen, W. Dahmen, R. DeVore, G. Petrova, P. Wojtaszczyk *Convergence rates for greedy algorithms in reduced basis methods.* 2011.

[2] A. Buffa, Y. Maday, A.T. Patera, C. Prudhomme, and G. Turinici, *A Priori convergence of the greedy algorithm for the parameterized reduced basis.* 2012.

Introduction to the NIRB methods

Reduced basis methods

- Optimization over parameter space
- High Fidelity (HF) real-time simulations

Non-Intrusive Reduced basis methods (NIRB)

Industrial context $\rightarrow$ **black box solver**

A model problem

Introduction to the two-grid method within the parabolic context

A model problem

$$\begin{cases} u_t - \mu \Delta u = f, \text{ in } \Omega \times]0, T], \\ u(\mathbf{x}, 0) = u_0(\mathbf{x}), \text{ in } \Omega, \\ u = 0, \text{ on } \partial\Omega, \ \forall t \in [0, T], \end{cases}$$

- $\mu \in \mathbb{R}$: Variable parameter
- $u(\mathbf{x}, t; \mu)$: Unknowns
  - $u_h^n \in V_h$ on the fine mesh $\mathcal{T}_h$ and fine time grid F_n (HF),
  - $u_H^m \in V_H$ on the coarse mesh $\mathcal{T}_H$ and coarse time grid G_m.

1. Offline stage: $u_h((\mu, t^n)_i)$: Snapshots on $\mathcal{T}_h$
2. Online stage: $u_H(\mu, \tilde{t}^m)$: Solution on $\mathcal{T}_H$ $(H^2 \sim h)$

[3] R. Chakir, Y. Maday, *A two-grid finite-element/reduced basis scheme for the approximation of the solution of parameter dependent PDE.* 2009.

[4] E. Grosjean, Y. Maday, *error estimate of the non-intrusive reduced basis method with finite volume schemes.* 2021.

[5] E. Grosjean, Y. Maday, *A doubly reduced approximation for the solution to PDE's based on a domain truncation and a reduced basis method: Application to Navier-Stokes equations.* 2022.

NIRB approach

The NIRB two-grid method is applied with two different time schemes.

Decomposition

Separation of variables

$$u_h(\mathbf{x}, t; \mu) = \sum_{j=1}^{N} a_j^h(\mu, t^n)\, \Phi_j^h(\mathbf{x}),$$

$(\Phi_j^h)_{j=1,\dots,N} \in X_h^N$: L^2-orthonormalized basis functions (modes)

Coefficients $a_j^h(\mu, t^n)$

- Optimal coefficients: $(u_h(\mu, t^n), \Phi_j^h(\mathbf{x}))$,
- Our choice: $(u_H(\mu, \tilde{t}^m), \Phi_j^h(\mathbf{x}))$, with $(\Phi_j^h)_{j=1,\dots,N}$ L^2 & H^1-orthogonalized

NIRB – OFFLINE/ONLINE

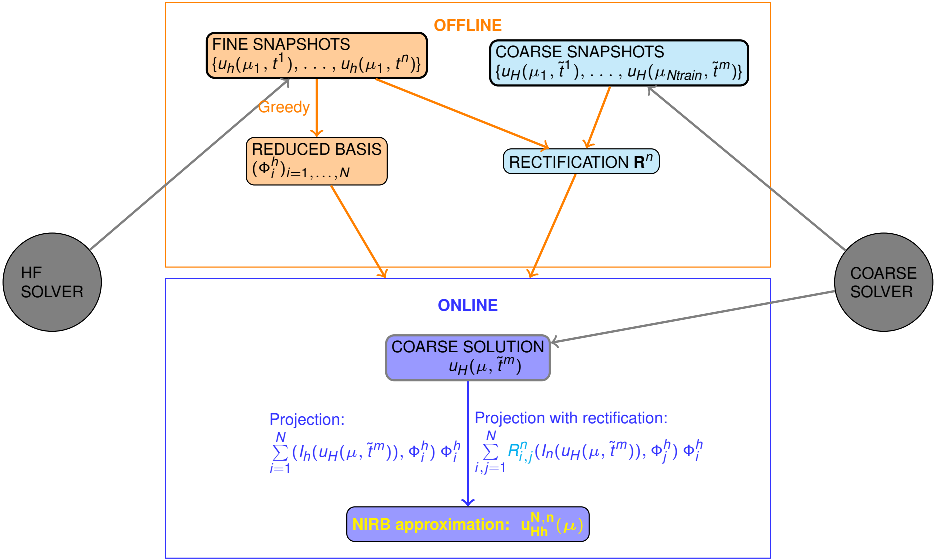

Greedy algorithm

$\rightarrow L^2$ orthonormalization.
$+$ Eigenvalue problem: $\forall v \in X_h^N, \int_\Omega \nabla\Phi_h \cdot \nabla v = \lambda \int_\Omega \Phi_h \cdot v$
$\rightarrow L^2(\Omega)$ and $H^1(\Omega)$ orthogonalization.

$$\mathbf{X_h^N} = \mathbf{Span}\{\Phi_1^h, \dots, \Phi_N^h\}$$

Greedy algorithm

for $k = 1, \dots, N$:

$$\widetilde{\mu}_k = \underset{\mu \in \mathcal{G}, n=\{0,\dots,\frac{T}{\Delta t_F}\}}{\arg\max} \frac{\left\| u_h(\mu,t^n) - P^{k-1}(u_h(\mu,t^n)) \right\|}{\left\| u_h(\mu,t^n) \right\|}$$

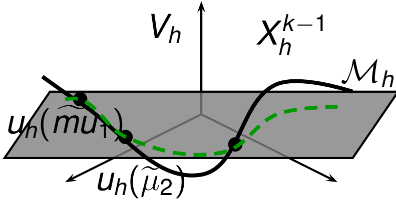

[6] J. Papez, U. Rüde, M. Vohralík, B. Wohlmuth. *Sharp algebraic and total a posteriori error bounds for h and p finite elements via a multilevel approach.* 2017.

FEM Error estimates

Energy error estimate with P_1 FE (parabolic equations)

$$\forall n, \left\| u(t^n)(\mu) - u_{Hh}^{N,n}(\mu) \right\|_{H^1(\Omega)} \leq \overbrace{\varepsilon(N)}^{T_1} + \underbrace{C_1 h + C_2 \Delta t_F}_{T_2} + \overbrace{C_3(N)H^2 + C_4(N)\Delta t_G^2}^{T_3},$$

$$\sim \mathcal{O}(h) + \mathcal{O}(\Delta t_F) \text{ if } H^2 \sim h \text{ and } \Delta t_G^2 \sim \Delta t_F,$$

where C_1, C_2 are constants independent of h and H. [7]

[7] V. Thomee. *Galerkin finite element methods for parabolic problems.* 2007

FEM Error estimates

Energy error estimate with P_1 FE (parabolic equations)

$$\forall n, \left\| u(t^n)(\mu) - u_{Hh}^{N,n}(\mu) \right\|_{H^1(\Omega)} \leq \overbrace{\varepsilon(N)}^{T_1} + \underbrace{C_1 h + C_2 \Delta t_F}_{T_2} + \overbrace{C_3(N) H^2 + C_4(N) \Delta t_G^2}^{T_3},$$

$$\sim \mathcal{O}(h) + \mathcal{O}(\Delta t_F) \text{ if } H^2 \sim h \text{ and } \Delta t_G^2 \sim \Delta t_F,$$

where C_1, C_2 are constants independent of h and H. [7]

Crank-Nicholson L^2 estimate (P_1 FE).

$\forall m \geq 0,$

$$\left\| u(t^m) - u_H^m \right\|_{L^2(\Omega)} \leq C H^2 \left[\|u_0\|_{H^2(\Omega)} + \int_0^{t^m} \|u_t\|_{H^2(\Omega)} \, ds \right] + C \Delta t_G^2 \int_0^{t^m} \left(\|u_{ttt}\|_{L^2(\Omega)} + \|\Delta u_{tt}\|_{L^2(\Omega)} \right) ds.$$

[7] V. Thomee. *Galerkin finite element methods for parabolic problems.* 2007

Numerical results with FEM

$f(t,\mathbf{x}) = 10[x^2(x-1)^2y^2(y-1)^2 - 2t((6x^2-6x+1)(y^2(y-1)^2)+(6y^2-6y+1)(x^2(x-1)^2))]$,

$\mu \in (0,10]$

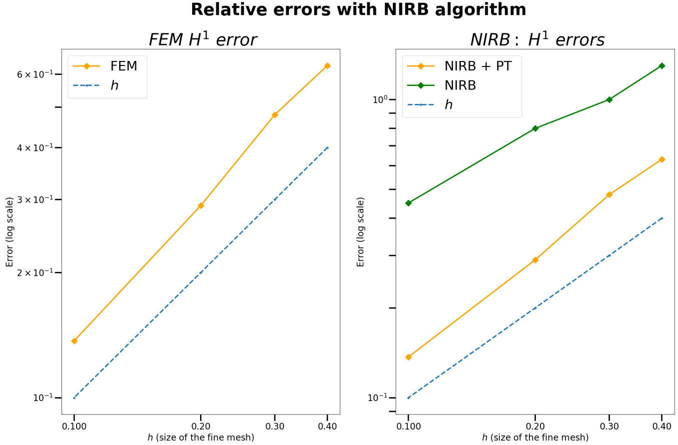

Figure: Test with $Ntrain = 10, \mu = 1, h \simeq \Delta t_F$

Numerical results with FEM

$$f(t,\mathbf{x}) = 10[x^2(x-1)^2y^2(y-1)^2 - 2t((6x^2-6x+1)(y^2(y-1)^2) + (6y^2-6y+1)(x^2(x-1)^2))],$$

$\mu \in (0, 10]$.

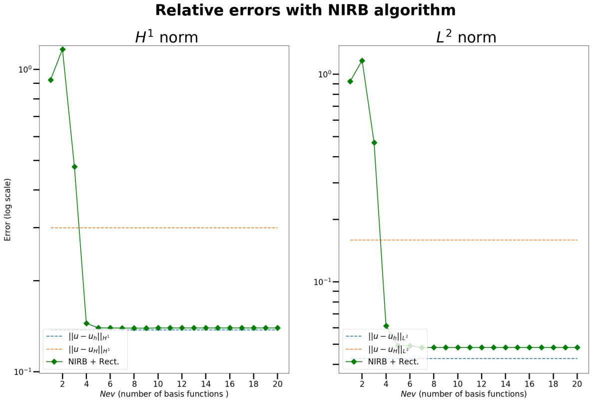

Figure: Test with $L^\infty(0,T;H^1(\Omega))$ (left) and $L^\infty(0,T;L^2(\Omega))$ (right) relative errors with a new parameter $(a,b)=(2,4)$, $T=5$, $\Omega=[0,1]\times[0,1]$

Numerical results with FEM

$$f(t,\mathbf{x}) = 10[x^2(x-1)^2y^2(y-1)^2 - 2t((6x^2-6x+1)(y^2(y-1)^2) + (6y^2-6y+1)(x^2(x-1)^2))],$$

$\mu \in (0, 10]$.

NIRB rectified error	$\max_{n=1,\dots,T/\Delta t_F} \frac{\left\| u_h(n\Delta t_F)(\mu) - u_{hh}^{N,n}(\mu) \right\|_{H_0^1}}{\left\| u_h(n\Delta t_F)(\mu) \right\|_{H_0^1}}$	$\max_{n=1,\dots,T/\Delta t_F} \frac{\left\| u_h(n\Delta t_F)(\mu) - u_H(n\Delta t_F)(\mu) \right\|_{H_0^1}}{\left\| u_h(n\Delta t_F)(\mu) \right\|_{H_0^1}}$
0.06	2.31×10^{-10}	6.84

Table: Maximum H^1 error over the parameters $[\mu = 10]$ (compared to the true NIRB projection and to the FEM coarse projection) with $N = 20$

Numerical results

NIRB approximations at time n=0,4,7,10

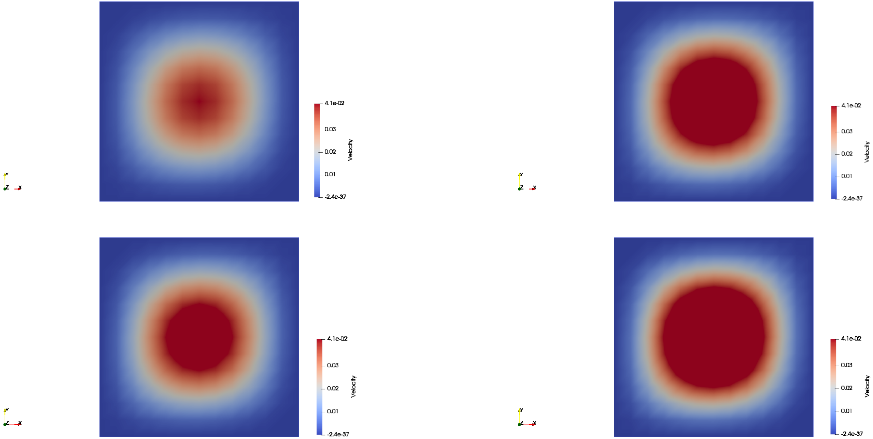

Numerical results

Table: FEM runtimes

FEM high fidelity solver	FEM coarse solution
00:03	00:02

Table: NIRB runtimes ($N = 18$)

NIRB Offline	classical rectified NIRB online
1:45	00:02

Brusselator equations

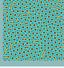

$$\partial_t u = a + uv^2 - (b+1)u + \alpha \Delta u$$
$$\partial_t v = bu - uv^2 + \alpha \Delta v.$$

- $(u(\mathbf{x}, t; \boldsymbol{\mu}), v(\mathbf{x}, t; \boldsymbol{\mu}))$: Unknowns
- $\boldsymbol{\mu}$=(a,b,α) $\in \mathbb{R}^3$: Variable parameter

Brusselator equations

$a = 2,\ b = 4 \in (0,5)$.

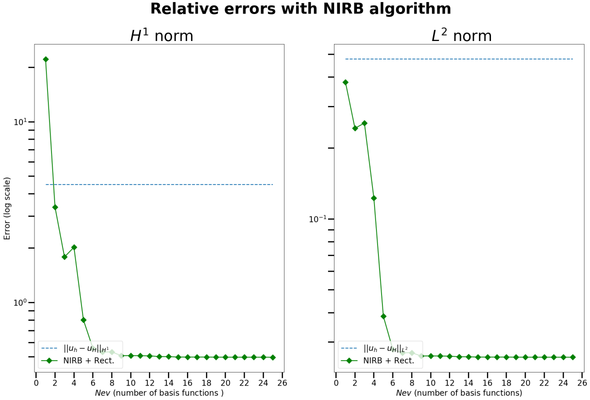

Figure: Test with $L^\infty(0,T;H^1(\Omega))$ (left) and $L^\infty(0,T;L^2(\Omega))$ (right) relative errors with a new parameter $\mu = 1$, $T = 2$, $\Omega = [0,1] \times [0,1]$

Brusselator equations

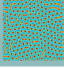

$a = 2, \; b = 4 \in (0, 5).$

NIRB rectified error	$\max\limits_{n=1,\dots,T/\Delta t_F} \frac{\left\| u_h(n\Delta t_F)(\mu) - u_{hh}^{N,n}(\mu) \right\|_{H_0^1}}{\left\| u_h(n\Delta t_F)(\mu) \right\|_{H_0^1}}$	$\max\limits_{n=1,\dots,T/\Delta t_F} \frac{\left\| u_h(n\Delta t_F)(\mu) - u_H(n\Delta t_F)(\mu) \right\|_{H_0^1}}{\left\| u_h(n\Delta t_F)(\mu) \right\|_{H_0^1}}$
0.5	1.3×10^{-9}	4.5

Table: Maximum H^1 error over the parameters [$\mu = 10$] (compared to the true NIRB projection and to the FEM coarse projection) with $N = 20$

Conclusions & Perspectives

- Error estimates of the NIRB 2-grid method with parabolic problems
- Development of two new NIRB tools

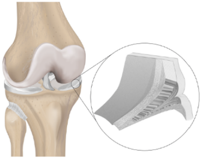

Figure: Meniscus tissue

TECHNISCHE UNIVERSITÄT KAISERSLAUTERN

Perspectives

- Two-grid a-posteriori error estimates

Conclusions & Perspectives

- Error estimates of the NIRB 2-grid method with parabolic problems
- Development of two new NIRB tools

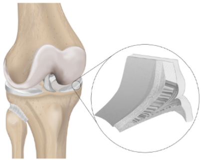

TECHNISCHE UNIVERSITÄT KAISERSLAUTERN

Figure: Meniscus tissue

Perspectives

- Two-grid a-posteriori error estimates

Merci pour votre attention!